

Preliminary evaluation of atmospheric mapping functions based on numerical weather models

A. E. Niell
Haystack Observatory

Abstract

Mapping of the zenith hydrostatic delay at radio frequencies to elevations as low as 3° has been improved by making use of the in situ atmosphere state. This information might be obtained from a numerical weather model, thus providing better atmosphere calibration on a global scale. The new model has been evaluated by comparing the repeatability of the lengths of baselines measured by Very Long Baseline Interferometry for a limited set of high accuracy experiments from 1994 January. The improvement compared to using the Niell (1996) mapping function, though significant, is less than expected, indicating other sources of unmodeled error.

1. Introduction

The space geodetic techniques of Very Long Baseline Interferometry (VLBI) and the Global Positioning System (GPS), whose capabilities have been significantly enhanced in order to make accurate studies of the solid earth, are now recognized for their potential contributions to atmosphere research in both weather prediction and climate. The observations of both techniques are affected by the additional propagation delay through the neutral atmosphere, and it is this excess delay that provides information on the amount of water vapor in the atmosphere that is of such importance to the meteorologists.

The information on integrated water vapor is obtained by estimating the related quantity, atmospheric delay, simultaneously with the other quantities of interest, such as station location and radio source positions (VLBI) or satellite orbits (GPS). VLBI and GPS are used to observe extraterrestrial sources of radio emission, one natural and one man-made. The signals are affected by the atmosphere, and the effect must be modeled. A parameterized relation in time and space is assumed so that few enough unknowns remain to leave the problem well-determined. The delay of the radio signal by the atmosphere has a basic dependence on the elevation for each antenna and is allowed to

change with time with a “correlation” of many observations. The elevation dependence is traditionally called the mapping function and is separated into the hydrostatic and wet components (Davis et al 1985). An additional dependence on azimuth has been found to agree with expectations from weather models (Chen and Herring 1997, MacMillan and Ma 1994) and to reduce the postfit residuals.

The quality of the results depends on the accuracy of both the apriori model and the partial derivatives for the estimated parameters. In the case of the atmosphere the apriori estimate is usually the hydrostatic component, which depends on the hydrostatic mapping function (the model) and hydrostatic delay (either based on measured pressure or modeled). The partial derivative is the wet mapping function (Davis et al., 1985).

Improvements in the atmosphere mapping functions have resulted in significant advances in the accuracy of the geodetic results (Davis et al., 1985; Niell, 1996). The functional form of the dependence of the atmosphere delay on elevation has, from the earliest days, been a continued fraction in $1/\sin(e)$. The evolution has been in the number of terms that define the continued fraction and in the nature of the parameters. At various times the parameters have been some combination of constants and functions of geographic location, local meteorological conditions and season.

In this article I present preliminary evaluation of a hydrostatic mapping function that has a new dependency for its parameters and that illustrates an important interplay of atmosphere models and measurements of the solid earth. The use of in situ data from a numerical weather model, summarized in the next section, provides a significant improvement in the mapping function (Niell, 2001). The improvement of the wet mapping function used as the partial derivative is not expected to be significant unless the spatial resolution is reduced from the current global gridded scale of $\sim 2^\circ$. (The effect of the wet mapping function is not evaluated in this paper.)

2. The basis for the new mapping functions

Marini (1972) showed that, for a spherically symmetric distribution of atmospheric refractivity, the ratio of the excess path delay at geometric elevation e , i.e. the vacuum elevation, to the path delay in the zenith direction can be approximated by a continued fraction of the form

$$m(e) = \frac{1 + \frac{a}{1 + \frac{b}{1 + c}}}{\sin(e) + \frac{a}{\sin(e) + \frac{b}{\sin(e) + c}}}$$

The numerator is included to normalize the fraction at an elevation angle of 90° , and the number of terms should be determined by the desired accuracy of the fit. Niell (1996) found that three terms is sufficient for elevations down to 3° . $m(e)$ is called the mapping function. The functional form and dependence of the parameters a , b , c , ... must be found that best match the actual variation of the mapping function for real atmospheres at arbitrary locations and times.

As the accuracy of the VLBI and GPS observations has improved, the accuracy required of the atmosphere model has increased. Early mapping functions used constant values for the parameters and only one or two terms (Chao, 1974). The importance of including the dependence on location of the site and on the current state of atmosphere, characterized by the use of surface meteorological data, was next established (Lanyi, 1984; Davis et al., 1985; Ifadis, 1986; Herring, 1992). However, Niell (1996) recognized from the studies of Herring (1992) that since the mapping function is an integral quantity through the neutral atmosphere, surface information might lead to a bias, especially in winter at high latitudes.

The ideal method for obtaining the mapping functions (for an azimuthally symmetric atmosphere) would make use of vertical profiles of refractivity at each site to calculate the mapping functions explicitly by raytracing. However, since such data are available at very few sites, Niell (1996) suggested parameterizing the mapping function coefficients

in terms of the site latitude and the day-of-year. This proposal was based on studies of mapping functions calculated from radiosonde data for a large number of locations which indicated that seasonal properties of the atmosphere are more representative than surface measurements for overall accuracy.

The limitation of a day-of-year based mapping function, which does provide greater accuracy both seasonally and when averaged over a year compared to using surface data, is that the short term (sub-daily to weekly) variations are not represented. To reproduce these changes, in situ information on the state of the atmosphere is needed. Niell (2001) has shown that data from global numerical weather models can be used to provide this information. For the hydrostatic component there is a strong correlation between the geopotential height of the 200 hPa pressure level and the mapping function. Thus the geopotential height at this pressure level, which is a product of most numerical weather analyses, can be interpolated in latitude and longitude and, along with the latitude of the site, used as the input parameters for the hydrostatic mapping function. A correction is made for the height of the site above sea level using the algorithm of Niell (1996). For the wet component the temperature and water vapor density profiles are used to calculate a "pseudo-mapping function" wet parameter which is then used in the coefficients of the wet mapping function. The parameter is the ratio of the integral of wet refractivity along a geometric path at an elevation of 3° to the integral of the wet refractivity in the zenith direction. The wet parameter is calculated at the grid points of the numerical weather analysis nearest the site and then interpolated to the site position. The mapping functions using coefficients determined by this procedure are designated IMFh and IMFw for the hydrostatic and wet components, respectively. (IMF stands for Isobaric Mapping Function.)

The new mapping functions were evaluated using radiosonde data taken at 0 UT and 12 UT for 26 globally distributed sites for the year 1992 (Niell, 2001). The vertical profiles of temperature, pressure, and relative humidity were used to calculate the hydrostatic and wet mapping functions at 5° . These were compared to the mapping functions calculated as described above using the gridded global weather model data

from the re-analysis by the Goddard Space Flight Center Data Assimilation Office (DAO) (Schubert, Pjaendtner, and Rood, 1993). Assuming that the mapping functions calculated from the radiosonde profiles represent the "true" values, the mean differences and standard deviations between IMFh and IMFw and their "true" values for the 26 sites are a measure of the error that will be introduced by using the analytic mapping functions. Since "mapping function units" are not readily visualized, conversion to equivalent estimated height uncertainty can be made. Using the rule of thumb that the height uncertainty is approximately one-third of the delay error at the lowest observed elevation, and assuming a zenith delay of 2300 mm, the height uncertainty due to the hydrostatic mapping function error for each of the twenty-six sites is shown in Fig. 1. The height uncertainty due to the wet mapping function error, also shown in Fig. 1, is calculated using the actual zenith wet delay to multiply the mapping function standard deviation. For comparison the expected uncertainties using a currently popular mapping function, NMF (Niell, 1996), are also shown. Even though the uncertainty of the scaling is perhaps twenty percent, the two mapping functions, IMF and NMF, are affected the same way, so the relative performance is preserved. Two important results are evident from this figure: 1) the error in the estimation of height due to errors in the hydrostatic mapping function dominates that due to the wet mapping function outside of the tropics; 2) the height uncertainty from the combined effects of IMFh and IMFw is about half that of NMF. Although it is not shown, IMFw provides about a twenty-five percent improvement over NMFw.

This comparison with mapping functions based on actual in situ atmospheric data from radiosondes demonstrates that a significant improvement in modeling the atmosphere for geodetic applications can be made for sites anywhere on earth by using the gridded data of a global numerical weather model. Because of the correlation of the height estimate and the atmosphere delay, the improvement will be effective for the meteorological applications also.

The magnitude of the expected height uncertainty is related to the minimum elevation of the data used in the estimation. The results in Fig. 1 are for 5°. For 7° minimum

elevation the values would be about fifty percent of those shown in Fig.1 For 10° and 15° the fractions are about twenty percent and about five percent.

3. Evaluation of the new hydrostatic mapping function using VLBI data

Having demonstrated by comparison with real atmosphere data that the new atmosphere models are better, the next step is to apply them to geodetic data. If the atmosphere mapping functions are the primary source of error, then changing to the new model will reduce the standard deviation of the geodetic estimates of the local vertical of the site locations. A stringent test of this expectation is comparison of VLBI baseline length measurements using NMF and IMF. For a change in site height, Δh , the baseline length change is

$$\Delta L = \Delta h \cdot B / 2R$$

where B is the baseline length and R is the radius of the Earth. Since baseline lengths are invariant to rotations, comparisons are not sensitive to errors in estimated earth orientation parameters. VLBI data are useful for comparison because MacMillan and Ma (1994) and Niell (1996) have shown that improvements in baseline length repeatability continue down to at least 8° minimum elevation. GPS data are not suitable for such an evaluation because the geodetic results for observations below about 15° are dominated by other error sources, such as orbit errors and multipath and scattering related to the antenna and site environment (Elosegui et al 1995).

For this preliminary evaluation a set of VLBI experiments from 1994 January has been used. These observations, designated CONT94, provided almost continuous coverage (twelve out of thirteen days) with the same network of antennas. The global distribution of the sites (Wetzell, Germany; Onsala, Sweden; Westford, Massachusetts; Ft. Davis, Texas; Los Alamos, New Mexico; Fairbanks, Alaska; and Kokee, Hawaii) included baseline lengths from 600 km to 10,000 km, ensuring adequate separation of the height corrections and the atmosphere delays in the estimation process. The altitudes of the sites ranged from sea level to 1600 m. Except for Hawaii, the sites are at latitudes greater than 30°. The minimum elevation of observations was 5°. For the comparisons described here, atmospheric gradients were also estimated. The estimation program used

was *solvk* (Herring et al, 1990). Separate baseline lengths were estimated for each 24-hour period. For the baseline length repeatability test, two analyses were made, differing only in the hydrostatic mapping functions. The NMF wet mapping function was used for both analyses. Although the effects of ocean loading were included, no corrections were made for atmosphere pressure loading. The latter can cause vertical displacements of several millimeters RMS for continental sites.

The results are shown in Fig. 2. The solid line describes the expected standard deviation if the vertical error at all sites were 8 mm, corresponding to the mid-latitude uncertainty expected from NMFh. The dashed line is for a total vertical error of 4 mm, which might be attained if the dominant error were due only to the mis-modeling of IMFh. For either of the solutions the error due to the wet mapping function is less than 2 mm.

The results using IMFh indicate clearly that the mapping functions are not the principal source of error for these experiments, since the standard deviations do not approach the line corresponding to the inherent accuracy of the mapping function ($\sigma_v = 4$ mm). However the use of IMFh is clearly an improvement over NMFh. As one indication, more than twice as many baselines have better repeatability when using IMFh. For another, the standard deviations of seven baselines are improved by more than 0.5 mm, while only two are made worse than this amount. (A more quantitative assessment will be made using one or more years of data.)

This comparison has two significant limitations. Only two weeks of the year are covered by the observations, and these occur in the winter. For sites outside of the tropics the variation in hydrostatic mapping function is much larger in winter than summer, suggesting that the differences observed may be among the largest. On the other hand, the corrections for such a short period may not sample the periods of largest error. The other limitation is the lack of correction for atmospheric pressure loading. Chen and Herring (1997) concluded that much of the residual vertical error after modeling for atmospheric gradients at the Westford site for this same period might be due to pressure loading.

In order to illustrate the magnitude of the effect of the change of mapping function on the estimation of the zenith wet delay another solution was made. The hydrostatic mapping function for only Onsala was changed from IMFh back to NMFh. The differences in the estimates of zenith wet delay for Onsala that arise from the change in hydrostatic mapping function are shown in Fig. 3. The change, which varies from -3 mm to $+6$ mm of zenith wet delay in this thirteen day period, is however only a measure of the difference, and the figure gives no indication of which mapping function is correct. To evaluate which mapping function is more likely to be correct, each series of zenith wet delays was compared with measurements for the same period by the Astrid microwave water vapor radiometer at Onsala (Emardson et al 1999). Unfortunately, the evaluation is inconclusive for two reasons. First, when all of the data are interpolated to common points and differenced, the mean differences, $ZWD(IMFh)-ZWD(WVR)$ and $ZWD(NMFh)-ZWD(WVR)$, are not significantly different, having values of -0.9 mm and -1.2 mm, respectively, with an uncertainty in the mean difference of 0.14 mm. The standard deviations of the differences are 7.9 mm and 8.0 mm, which are not significantly different either. The second reason the comparison is compromised is that a small amount of the WVR data are contaminated by liquid water on the optics, and these data contribute a significant amount of the standard deviation. When the wet mapping function has been implemented, the comparison will be improved by including a longer time span of common data and by using more stringent filtering of contaminated WVR data.

This is the first stage of testing the new mapping functions. Clearly, the wet mapping function must also be included. The next step will be to evaluate the change in baseline length repeatability for at least one year of data (preferably several) to see if there is a significant improvement that persists over all seasons and for a more global distribution of sites. Before such a comparison is made, the model in *solvk* must be amended to include atmosphere pressure loading.

4. Numerical weather model considerations

These initial results make use of the DAO assimilated data set, which has a grid spacing of 2° by 2.5° in latitude/longitude. The error in the mapping function due to interpolation of the geopotential height of the 200 mb isobar is negligible compared to the uncertainty in the height in the assimilation itself (Schubert et al., 1993). The error due to the geopotential height uncertainty will not be reduced by using a smaller grid spacing unless the accuracy is improved. Even then the error might be due to the variability of the atmosphere above the 200 mb height. Using the 100 mb height did not improve agreement with the radiosonde however.

Although not discussed in this paper, the lack of improvement in the wet mapping function is most likely due to the coarse horizontal grid of the profile data from the DAO assimilation. Similar data on much finer grids are available for selected areas of the world by various meteorological agencies, although not on a global scale. For specific areas it is of interest to evaluate the possible improvement in the wet mapping function that might be obtained from having profile information closer to the site.

Acknowledgments

I am grateful to the organizers of the COST Action 716 Workshop for the invitation to participate in such an interesting and productive meeting. Additional support was provided by National Aeronautics and Space Administration Grant NAG5-6063.

I thank Gunnar Elgered for providing the Astrid water vapor radiometer data.

References

- Chao, C. C., The tropospheric calibration model for Mariner Mars 1971, JPL Technical Report 32-1587, 61-76, 1974.
- Chen, G. and T.A. Herring, Effects of atmospheric azimuthal asymmetry on the analysis of space geodetic data. *J. Geophys. Res.*, 102, B9, 20,489-20,502, 1997.
- Davis, J. L., T. A. Herring, I. I. Shapiro, A. E. E. Rogers, and G. Elgered, Geodesy by radio interferometry: Effects of atmospheric modeling errors on estimates of baseline length, *Radio Science*, 20, 1593-1607, 1985.

- Elósegui, P., J. L. Davis, R. T. K. Jaldehag, J. M. Johansson, A. E. Niell, and I. I. Shapiro, Geodesy using the global positioning system: The effects of signal scattering on estimates of site position, *J. Geophys. Res.*, **100**, 9921-9934, 1995.
- Emardson, T. Ragne, G. Elgered, and J. M. Johansson, External Atmospheric corrections in geodetic very-long baseline interferometry, *J. Geodesy*, **73**, 373-383, 1999.
- Herring, T. A., Modeling Atmospheric Delays in the Analysis of Space Geodetic Data, in Symposium on Refraction of Transatmospheric Signals in Geodesy, J. C. DeMunk and T. A. Spoelstra, eds., Netherlands Geodetic Commission Series No. 36, 157-164, 1992.
- Herring, T. A., J. L. Davis, and I. I. Shapiro, Geodesy by radio interferometry: The application of Kalman filtering to the analysis of very long baseline interferometry data, *J. Geophys. Res.*, **95**, 12,561-12,581, 1990.
- Ifadis, I., The atmospheric delay of radio waves: modeling the elevation dependence on a global scale, Technical Report No. 38L, School of Electrical and Computer Engineering, Chalmers University of Technology, Gothenburg, Sweden, 1986.
- Lanyi, G., Tropospheric Delay Effects in Radio Interferometry, TDA Progress Report 42-78, vol. April-June 1984, Jet Propulsion Laboratory, Pasadena, California, 152-159, Aug 15, 1984 (the sign of F_{bend4} was misprinted in this paper).
- MacMillan, D. S., and C. Ma, Evaluation of very long baseline interferometry atmospheric modeling improvements, *J. Geophys. Res.*, *99(B1)*, 637-651, 1994.
- Marini, J. W., Correction of satellite tracking data for an arbitrary tropospheric profile, *Radio Science*, *7*, 223-231, 1972.
- Niell, A. E., Global mapping functions for the atmosphere delay at radio wavelengths, *J. Geophys. Res.*, *100*, 3227-3246, 1996.
- Niell, A. E., Improved atmospheric mapping functions for VLBI and GPS, *Earth, Planets, and Space* (accepted), 2001.
- Schubert, S. D., J. Pjaendtner, and R. Rood, An assimilated data set for Earth science applications, *B. A. M. S.*, *74*, 2331-2342, 1993.

Figures

1. Standard deviation of apparent height for the combined errors of the hydrostatic and wet mapping functions. The dashed lines are of the form $\cos(2 \times \text{latitude})$ and are intended

only to guide the eye to the expected height uncertainties for the combined hydrostatic and wet mapping function errors for IMF and for NMF. Except at very low latitudes the error due to the wet mapping function is insignificant. (IMFw - plus sign; IMFh - cross; IMFw + IMFh - open circle; NMFw+NMFh - asterisk).

2. Standard deviation of baseline lengths for VLBI data in CONT94 using NMFh (circles) or IMFh (crosses)
3. Difference in estimates of zenith wet delay by VLBI for Onsala in the sense $ZWD(IMFh) - ZWD(NMFh)$

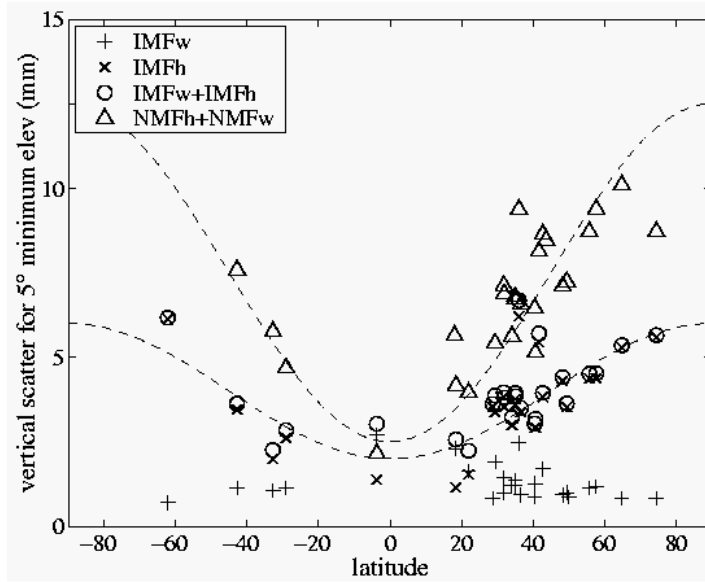


Figure 1

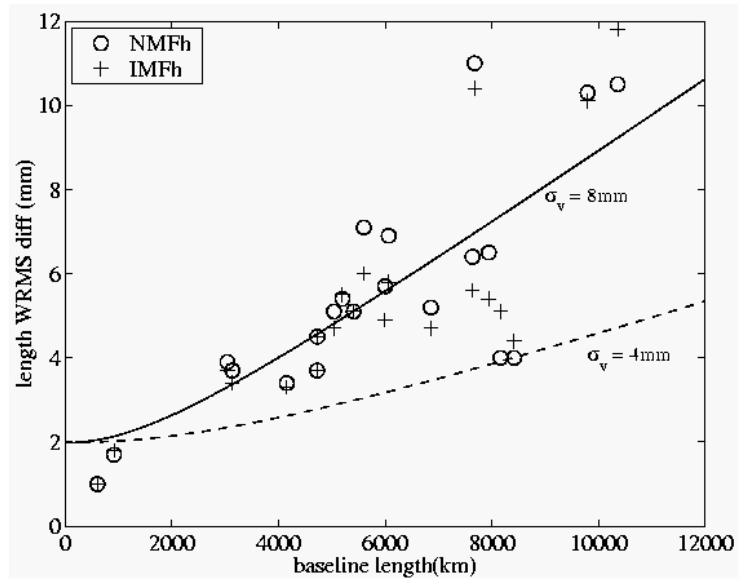


Figure 2

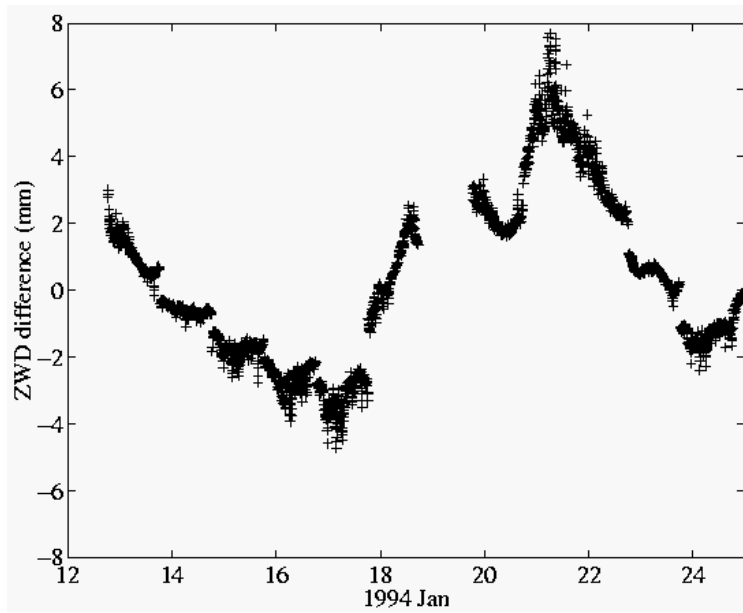


Figure 3